Second-order nonlinear optical properties of bond-alternating dipolar structures

Y. M. Cai, S. Yamada,* O. Zamani-Khamiri, and A. F. Garito
Department of Physics and Astronomy and Department of Materials Science and Engineering, University of Pennsylvania, Philadelphia, Pennsylvania 19104

K. Y. Wong
Department of Physics, Chinese University of Hong Kong, New Territory, Hong Kong
(Received 6 August 1996; revised manuscript received 26 December 1996)

Second-order nonlinear susceptibilities of two dipolar quinoid molecules, DCNQI and TPHQ2, are calculated using extensive single- and double-excitation-configuration interaction (SDCI). In sharp contrast to polyene studies, no overcorrelation of the ground-state energy level is observed for either of the two structures, suggesting the adequacy of SDCI calculations for both the ground and one-photon states. The calculated second-order susceptibility of DCNQI is found to be in excellent agreement with the results of dc field-induced second-harmonic-generation measurements in solution and in Langmuir-Blodget films. The principal off-resonance electro-optic coefficient $\beta_{xxx}(-\omega;0,\omega)$ at 0.65 eV is calculated to be -3000×10^{-30} esu for TPHQ2, a 20-fold increase compared to the calculated value of -140×10^{-30} esu for DCNQI. [S0163-1829(97)03819-8]

I. INTRODUCTION

Nonlinear optical properties of organic compounds have been the subject of intense research activity in the past two decades. The reason for the focus on organic compounds is the many advantages they possess compared to inorganic structures with respect to optoelectronics device applications. Among these are their ultrafast- and broadband-electronic responses, low dielectric constants, and negligible one-photon and two-photon absorptions at wavelengths used for optical-fiber telecommunications. In addition, the structure of organic compounds is relatively easy to modify via synthetic routes to meet specific needs of electro-optic device technologies.

The advances made in the design and synthesis of suitable structures with large nonlinear optical coefficients have been, in large part, due to advances in the understanding of the microscopic origins of these phenomena by means of theoretical studies.[1–6] These studies have established that the large nonlinearities observed in conjugated organic structures are due to virtual excitations of π-electron states whose properties are determined primarily by the correlated motions of the π electrons due to repulsive Coulomb interactions. Therefore, electronic wave functions can provide an adequate description of a molecular state only if they incorporate these correlation effects in the description of the electronic motions. Self-consistent molecular-orbital (SCF-MO) procedures that include single- and double-excitation-configuration interaction (SDCI) to take account of the correlated motions of the electrons have proved very successful in obtaining reliable descriptions of π-electron virtual excitations. The development of this theoretical methodology has led to the calculation of the nonlinear optical properties of numerous organic structures, usually in excellent agreement with experimental data.

One example of the application of the SDCI method is an earlier calculation[7] of the second-order nonlinear optical coefficients of the dipolar-quinoid structure, DCNQI [2-(4-dicyanomethylene cyclohexa-2, 5-dienylidine)-imidazolidine], shown in Fig. 1, where many-electron quantum calculations successfully predicted the observed negative sign and identified the microscopic origin of this rare phenomenon.

Additional experimental data on DCNQI, which have subsequently become available, plus the renewed interest in extended quinoid structures[8] and the enhanced computing capabilities available at present have motivated a more complete calculation of the second-order optical response of DCNQI, as well as that of its three-ring analog, TPHQ2, shown in Fig. 2. These calculations provide a refinement of the previous theoretical results and further enhance our understanding of the microscopic origin of nonlinear optical effects in this class of organic structures.

II. THEORETICAL METHOD

The microscopic second-order polarization $p_i^{\omega_3}$ can be expressed as

$$p_i^{\omega_3}=\beta_{ijk}(-\omega_3;\omega_1,\omega_2)E_j^{\omega_1}E_k^{\omega_2}, \tag{1}$$

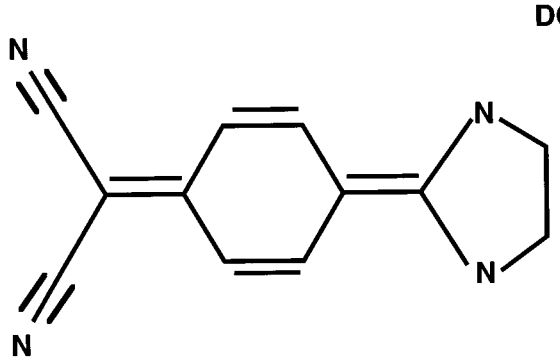

FIG. 1. Schematic molecular structure for DCNQI.

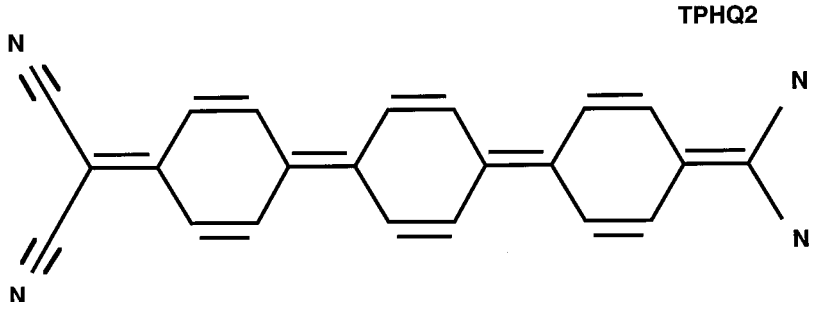

FIG. 2. Schematic molecular structure for TPHQ2.

where $\beta_{ijk}(-\omega_3;\omega_1,\omega_2)$ is the molecular second-order susceptibility. The analytical expression for the quantitative evaluation of β_{ijk} can be derived from time-dependent perturbation theory using a perturbation Hamiltonian of the form

$$H' = e\mathbf{r}\cdot\mathbf{E}^{\omega}, \tag{2}$$

describing the dipolar interaction of the molecular system with the electric field component of the electromagnetic field.

The second-order susceptibility tensor coefficients are then given by the following expression:[9]

$$\begin{aligned}\beta_{ijk}(-\omega_3;\omega_1,\omega_2) &= -\left(\frac{e^3}{2\hbar^2}\right)K(-\omega_3;\omega_1,\omega_2)\sum_{mn}{}' \frac{r^i_{gm}\overline{r^j}_{mn}r^k_{ng}}{(\omega_{mg}-\omega_3)(\omega_{ng}-\omega_2)} + \frac{r^i_{gm}\overline{r^k}_{mn}r^j_{ng}}{(\omega_{mg}-\omega_3)(\omega_{ng}-\omega_1)} \\ &+ \frac{r^k_{gm}r^{-j}_{mn}r^i_{ng}}{(\omega^*_{mg}+\omega_2)(\omega^*_{ng}+\omega_3)} + \frac{r^j_{gm}r^{-k}_{mn}r^i_{ng}}{(\omega^*_{ng}+\omega_1)(\omega^*_{ng}+\omega_3)} + \frac{r^k_{gm}r^{-i}_{mn}r^j_{ng}}{(\omega^*_{mg}+\omega_2)(\omega_{ng}-\omega_1)} + \frac{r^j_{gm}r^{-i}_{mn}r^k_{ng}}{(\omega^*_{mg}+\omega_1)(\omega_{ng}-\omega_2)}.\end{aligned} \tag{3}$$

The above equation, also known as the summation over states (SOS) equation, relates the second-order susceptibility tensors β_{ijk} to the t component of the transition-matrix element for states p and q, r^t_{pq} with $r_{pq}=\langle r-r_{gg}\rangle_{pq}$, and to the complex excitation energies $\hbar\omega_{ng}=\hbar w_{ng}-i\hbar\Gamma$, where Γ is a damping constant and $\hbar w_{ng}$ is the calculated transition energy from the ground state g to the excited state n. The factor K is a numerical constant the value of which depends on the nonlinear process and the prime on the summation denotes exclusion of the ground state as a summation index.

The reliability of the calculated second-order nonlinear response is seen to depend on the accuracy of the calculated molecular-optical transitions, i.e., the transition energies and the transition moments and, therefore, on the quality of the wave functions used in the evaluation of the transition moments and excitation energies. The wave functions used in this work were, therefore, as in our earlier DCNQI calculations, based on an all valence, semiempirical, (SCF-MO) calculation, in the rigid lattice CNDO/S (complete neglect of differential overlap/spectroscopy) approximation and configuration interaction (CI) with single and double excitations (SDCI) to account for electron correlation. The results of these calculations will be presented in the following sections for DCNQI and TPHQ2.

III. RESULTS AND ANALYSIS

A. DCNQI

In this section the results of recent calculations of the second-harmonic microscopic susceptibilities $\beta_{ijk}(-2\omega;\omega,\omega)$ of DCNQI are presented and compared to experimental data. The CI basis set consisted of the ground SCF configuration and all single and double excitations from the seven-highest occupied to the seven-lowest-unoccupied π molecular orbitals, i.e., a total of 1275 configurations. The SDCI eigenfunctions for the ground and the lowest 1274 excited π-electron states were calculated using the procedure described in the preceding section. Table I lists the calculated linear-optical transitions of the low-lying states.

Theoretical studies of polyenes have established that configuration interaction calculations limited to single and double excitations lead to ''overcorrelation'' of the ground state,[10] meaning that the ground state energy is lowered to a much larger extent compared to that of the one-photon states. Agreement with experimental gas phase spectra in polyenes is, therefore, achieved by empirical formulas that adjust for the ground-state overcorrelation.[11] In DCNQI, despite its polyenelike bond-alternated structure, however, the lowering of the $2\,^1A_1$ energy by 1.23 eV is comparable to, even somewhat larger than, that of the ground state that is lowered by

TABLE I. Calculated optical transitions of low-lying electronic states of DCNQ1.

State	$E(f)$ [eV(osc. str.)]	$\lvert\mu_{ng}^{x}\rvert$ (D)	μ_{n}^{x} (D)	$\Delta\mu_{n}^{x}$ (D)
$2\,^1A_1$	2.55(0.83)	9.29	13.56	−4.89
$1\,^1B_2$	3.65(0.01)	0.0	15.99	−2.43
$3\,^1A_1$	3.94(0.14)	3.12	11.45	−6.97
$4\,^1A_1$	4.69(0.02)	1.16	13.35	−5.07
$2\,^1B_2$	4.88(0.01)	0.0	16.39	−2.04

0.86 eV. No correction for ''overcorrelation'' of the ground state was, therefore, necessary in this case. The double summation of the SOS equation was performed using $\omega_2=\omega_1=\omega$ and included all of the calculated excited states.

The experimentally accessible microscopic second-order susceptibility is the vector part

$$\beta_x=\beta_{xxx}+\tfrac{1}{3}\sum_i(\beta_{xii}+2\beta_{iix}), \tag{4}$$

where the x axis is along the dipolar axis of the molecule and the summation index i represents the coordinates x,y,z.

Since the one-electron levels used in this calculation are all π molecular orbitals, they belong to either the a_2 or the b_1 representation of the molecular symmetry group C_{2v}. The calculated π-electron excited states are, therefore, either of A_1 or B_2 symmetry. There are no β_{xzz} or β_{zzx} contributions since in each term contributing to these tensor components there is at least one matrix element where the z operator couples the ground to an excited state. The z operator belongs to the B_1 representation of the C_{2v} point group and its matrix element connecting the ground state, which is of A_1 symmetry, and any excited state of A_1 or B_2 symmetry will be zero. The equation for β_x can, therefore, be written as

$$\beta_x=\beta_{xxx}+\tfrac{1}{3}(\beta_{xyy}+2\beta_{yyx}). \tag{5}$$

The component β_{xxx} is the major contributing term in DCNQI. At 0.65 eV for example, the gas phase calculated values are $\beta_{xxx}=-45.4$, $\beta_{xyy}=3.5$, and $\beta_{yyx}=2.9$, all in units of 10^{-30} esu. (esu=1 cm^4/statvolt.)

In each of the terms in the expression for β_{xxx} the x operator, which belongs to the A_1 representation of the molecular symmetry group, couples the totally symmetric ground state to an excited state. The only states that can contribute to β_{xxx} component must, therefore, also belong to the A_1 symmetry species. There are both diagonal, $m=n$, and off-diagonal contributions to β_{xxx}. The main diagonal term is due to the first excited state. The SOS equation shows that a large diagonal contribution to β_{xxx} requires that the transition moment μ_{ng}^{x} and the dipole moment difference $\Delta\mu_n^x=\mu_n^x-\mu_g^x$ of the contributing state be relatively large and its transition energy be relatively small. The first excited state of DCNQI satisfies all three conditions with calculated transition energy of 2.55 eV, transition moment of $\mu_{ng}^{x}=9.29$ D, and dipole moment difference $\Delta\mu^x=-4.87$ D. The main off-diagonal contributions to β_{xxx} are due to states with large dipole coupling, in the x direction, to the first excited state. This transition moment, μ_{1n}^{x}, is 5.09 D for the third excited state, $3\,^1A_1$, and 7.23 D for the $6\,^1A_1$ state, which is the ninth excited state. These two states, therefore, make relatively large off-diagonal contributions to β_{xxx}. It should be noted that, to a large extent, the off-diagonal contributions cancel each other leading to an even more prominent role of the first excited state. The components β_{xyy} and β_{yyx} contained in β_x are much smaller than β_{xxx} because the dipole moment difference between the ground and any excited state, $\Delta\mu_n$, has no y component due to the C_{2v} molecular symmetry. The diagonal contributions are, therefore, zero leaving only small off-diagonal matrix elements involving the y operator.

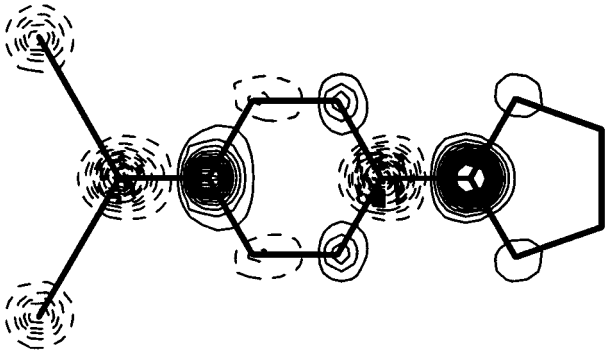

FIG. 3. Contour diagram of $\Delta\rho_{2\,^1A_1}$ for DCNQI. Solid and dashed lines correspond to increase and decrease, respectively, in electron density at 0.4 Å above the molecular plane.

Considering the above analysis, the microscopic origin of the negative sign of β_x is seen to be in the negative sign of $\Delta\mu$ of the first excited state. The dipole moments of the ground and the excited $2\,^1A_1$ state are both positive, as seen in Table I, i.e., in both states there is a build up to electronic charge on the electron withdrawing cyano (CN) groups and a corresponding depletion of charge on the amine side of the molecule. The dipole moment of the $2\,^1A_1$ state, however, is smaller by 4.87 D, i.e., there is a transfer of electronic charge from the acceptor CN groups to the donor amine side upon excitation to the $2\,^1A_1$ state. The charge redistribution in the course of a molecular-electronic-excitation on process is best described by the contour diagrams of the difference density function $\Delta\rho_n=\rho_n-\rho_g$, where ρ_m is the first-order reduced density matrix given by

$$\rho_m=\int\Psi_m^*(r_1,r_2,\ldots,r_N)\times\Psi_m(r_1,r_2,\ldots,r_N)dr_2\cdots dr_N. \tag{6}$$

The contour diagrams of $\Delta\rho_{2\,^1A_1}$ for DCNQI is shown in Fig. 3. It clearly shows the microscopic nature of the charge redistribution and the origin of the negative $\Delta\mu$ as due to the transfer of electronic charge from the acceptor region to the donor side of the molecule.

In order to compare the calculated value of β_x with experimental results the gas phase values have to be adjusted for the effect of solvent interactions and for the broadening of the absorption peak. The interactions with the solvent molecules induce a shift in the transition energies, known as

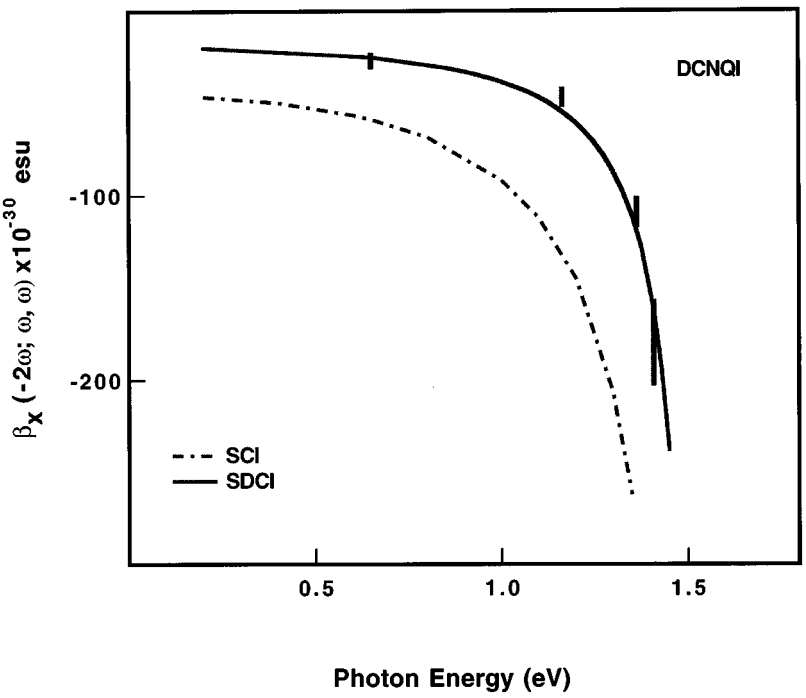

FIG. 4. Calculated off-resonance dispersion curves of β_x for DCNQI in DMSO compared to experimental DCSHG measurements: SDCI calculation (solid curve); SCI calculation (dashed curve); experimental data shown as error bars.

the solvatochromic shift. In the case of molecules whose excited state has a smaller dipole moment compared to their ground state the shift is towards an increase in the transition energy in solvents of increased polarity. The calculated dipole moment of DCNQI in its ground and first excited states are 18.42 and 13.56 D, respectively, i.e., there is a decrease of 4.87 D in the dipole moment of the molecule upon excitation to the first excited state. The transition energy in solution is, therefore, expected to be higher than that calculated for the isolated molecule. The calculated gas phase transition energy of the first excited state is 2.55 eV while the observed transition energy measured for a solution of DCNQI in dimethylsulfoxide (DMSO) has a higher value of 3.08 eV, as expected. This rather large solvent shift was taken in to account by increasing all transition energies by the amount of the solvent-induced shift of the first excited state and using this new set of values in the SOS equation to calculate the tensor components under experimental conditions. This is, of course, an approximation where it is assumed that all the excited states are affected identically in the solvent environment. The justification for this approximation is that the other states are at relatively much higher energies and have lower transition moments and, therefore, will have a much less impact on the calculated β_x value.

In Fig. 4 two calculated dispersion curves of β_x for DCNQI in DMSO are compared to the experimental values. The solid curve is the calculated values using SDCI wave functions while the dashed curve shows the SCI (single excitation configuration interaction) result. The agreement of the SDC calculation with the experimental dispersion measurements is seen to be excellent. The SCI calculation, however, overestimates the magnitude of β_x over the range of frequencies by at least a factor of 2. This indicates that single-excitation configurations alone do not adequately account for electron correlation and, therefore, the wave functions based on such calculations can give at best a rough description of the states. The excellent agreement between the SDCI calculation and the experimental measurements shows, on the other hand, that including the double excitation configurations is essential for obtaining wave functions that can adequately describe the electronic motions and lead to theoretical values of nonlinearity coefficients well within experimental errors.

The experimental measurements shown in Fig. 4 are at frequencies relatively far from the 2ω resonance. The theoretical dispersion curves shown were, therefore, calculated assuming zero linewidth. At near or on resonance frequencies, however, such calculations lead to divergence, as seen in Fig. 4. The calculation of tensors β_{ijk} at these frequencies were, therefore, carried out using Eq. (3) with the complex form for the transition energies. The damping constant was chosen to have a value of $\hbar\Gamma = 0.17$ eV, which is very close to the measured half-width of the linear absorption peak. The result of this calculation is shown in Fig. 5, where the calculated $|\beta_x|$ is compared to the dispersion measurements the second harmonic susceptibility of the Langmuir-Blodgett (LB) film[12] of the quinoid molecule.[13] The experimental results are seen to be in excellent agreement with the theoretical calculations. The experimental dispersion measurements in DMSO are also shown in Fig. 5. at each frequency. The SDCI calculation is thus seen to be remarkably accurate in reproducing the experimental results under a variety of physical conditions and over a large range of frequencies, both off and on resonance.

B. TPHQ2

The excellent agreement with experiment of the the SCF-MO-SDCI calculations of the second-order nonlinear optical response of DCNQI motivated the calculation of the electro-optic coefficients of the extended dipolar quinoid system TPHQ2 the structure of which is shown in Fig. 2. The parent

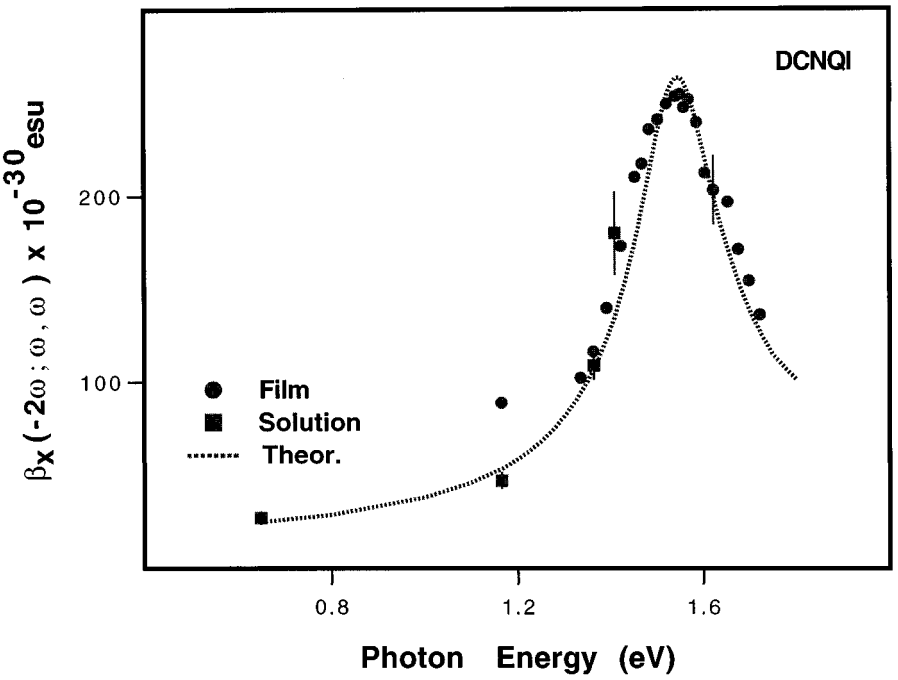

FIG. 5. Calculated SDCI dispersion curve (dotted curve) of the magnitude of $\beta_x(-2\omega;\omega,\omega)$ for DCNQI compared with DCSHG measurements in Langmuir-Blodgett films (full circles), and DCSHG measurements in DMSO (full squares). The average uncertainty in the LB film measurements and the uncertainties in the solution experiments are shown as error bars. An analysis of errors in second-order experiments can be found in Ref. 15.

compound, (3,3″), (5,5″)-tetra(*t*-butyl)-para-terphenoquinone (TPHQ), has been synthesized and its x-ray diffraction analysis has shown the molecule to be planar.[14] The TPHQ2 molecule was, therefore, also assumed to be planar with bond lengths consistent with the experimental bond lengths of the parent TPHQ and idealized bond angles of 120°. The x axis was again chosen to coincide with the molecular dipolar axis. The π-electron states were calculated using all single and double excitations from the eight-highest occupied to the eight-lowest unoccupied π molecular orbitals, i.e., a basis set of 2145 configurations.

The configuration interaction lowered the ground-state energy by 1.26 eV, which is comparable to the 1.45 eV lowering of the $2\,^1A_1$ state and, therefore, no correction for overcorrelation of the ground state was necessary in this case either. The calculated spectrum for the low-lying excited states are shown in Table II. The spectrum is seen to have shifted to lower energies by about 1 eV, compared to that of DCNQI, and both the $2\,^1A_1$ and the $3\,^1A_1$ states are seen to have gained appreciably in oscillator strengths in the TPHQ2 molecule. Otherwise, the two spectra are very similar. In each case, the spectrum is dominated by the transition from the ground to the first excited state and shows a relatively large gap of about 1.5 eV between the first two excited singlet A_1 states, which are the only states with appreciable oscillator strengths in the region of the spectrum below 5 eV.

TABLE II. Calculated optical transitions of low-lying electronic states of TPHQ2.

State	$E(f)$ [eV(osc. str.)]	$\lvert\mu^x_{ng}\rvert$ (D)	μ^x_n (D)	$\Delta\mu^x_n$ (D)
$2\,^1A_1$	1.73(1.64)	15.82	23.93	−15.62
$3\,^1A_1$	3.00(0.75)	8.11	24.40	−15.15
$4\,^1A_1$	3.27(0.10)	2.82	21.06	−18.49
$1\,^1B_2$	3.47(0.00)	0.0	18.12	−21.44
$5\,^1A_1$	3.95(0.10)	2.56	21.95	−17.60

The analysis of the second-order nonlinear response of TPHQ2 molecule reveals features that are qualitatively very similar to those found in DCNQ. The molecules TPHQ2 and DCNQI belong to the same symmetry point group and, since the x axis is along the molecular-dipolar axis in both cases, the analysis based on symmetry set forth above for DCNQI holds identically for TPHQ2. The main contribution to β_x is found to be, as in the case of DCNQI, due to the β_{xxx} component, the latter being more than two orders of magnitude larger than the xyy and the yxx components. As in the case of DCNQI, the only states that contribute to β_{xxx} are those belonging to the A_1 symmetry species. The diagonal part of β_{xxx} is dominated by the $2\,^1A_1$ state, its contribution being negative in sign and more than two orders of magnitude larger than that of the $3\,^1A_1$ state, the latter being the second largest contributing state. The largest off-diagonal contribution comes from the coupling of the $2\,^1A_1$ and $3\,^1A_1$ states. Also, as in the case of DCNQI, while there are numerous off-diagonal terms their overall contribution is relatively small due to cancellation of terms with opposing signs.

The above analysis of the contributing intermediate terms has shown the contribution of the virtual excitation sequence $1\,^1A_1 \rightarrow 2\,^1A_1 \rightarrow 2\,^1A_1 \rightarrow 1\,^1A_1$ to be larger than that of any other by at least two orders of magnitude. The magnitude of this term is directly dependent on the square of the moment for the $1\,^1A_1 \rightarrow 2\,^1A_1$ transition and on the magnitude of $\Delta\mu_1$ and inversely proportional to the transition energy of the $2\,^1A_1$. The sign of this contribution, however, is determined by the sign of $\Delta\mu_1$ at low frequencies, where the denominator is positive. The electronic charge redistribution upon excitation to the first excited state is shown in Fig. 6 as a density difference contour diagram. There is a redistribution of charge from the cyano end towards the amine end of the molecule with a net effect of a smaller dipole moment in

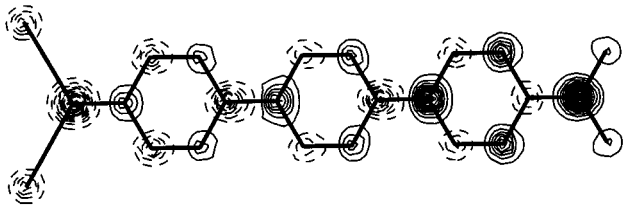

FIG. 6. Contour diagram of $\Delta\rho_{2\,^1A_1}$ for TPHQ2. Solid and dashed lines correspond to increase and decrease, respectively, in electron density at 0.4 Å above the molecular plane.

the $2\,^1A_1$ state. The dipole moment difference given by $\Delta\mu_n=\mu_n-\mu_g$ is, therefore, negative. The relatively large and negative $\Delta\mu$ of -15.6 D of the $2\,^1A_1$ state combined with its large transition moment of 15.8 D and low transition energy of 1.73 eV would, therefore, lead to a prediction of a relatively large and negative second-order susceptibility at below resonance frequencies, mainly due to the contribution of the above virtual-excitation sequence.

In Fig. 7 the results of dispersion calculations for β_{xxx} of TPHQ2 are shown. Since the first transition occurs at the relatively low energy of 1.73 eV, with the first second-harmonic resonance appearing at as low as 0.86 eV, the calculations presented are for the linear electro-optic coefficient $\beta_{xxx}(-\omega;0,\omega)$. In the absence of experimental data a damping constant of 0.2 eV was assumed. In Fig. 7 the real and imaginary parts as well as the magnitude of the electro-optic coefficient β_{xxx} are shown as a function of the applied frequency. At frequencies far from resonance β_{xxx} is seen to be almost purely real and negative with magnitudes of about 2000×10^{-30} esu. The real part of β_{xxx} is then seen to become increasingly negative with increasing frequency with values as high as -7000×10^{-30} esu at around 1.5 eV where the damping constant introduced in the SOS equations prevents divergence. The absolute value of β_{xxx} is seen to peak at about $36\,000\times10^{-30}$ esu at the ω resonance of the $2\,^1A_1$ state. Considering the calculated off-resonance $\beta_{xxx}(-\omega;0,\omega)$ for the two molecules at 0.65 eV, i.e., -140×10^{-30} esu for DCNQI and -3000×10^{-30} esu for TPHQ2, an enhancement of a factor of 20 is achieved in the nonlinear response of TPHQ2. Since the calculated dipole moment of TPHQ2 is larger than that of DCNQI by a factor of 2, the overall $\mu\beta$ of TPHQ2 will be enhanced by a factor of 40 compared to that of DCNQI.

IV. SUMMARY

The linear-optical transitions and second-order nonlinear susceptibilities of dipolar quinoid molecule DCNQI and its extended analog TPHQ2 have been calculated, using extensive basis sets of single and double excitation configurations. The calculated linear spectra for the two molecules show very similar characteristic features. Both spectra show a very strong low-lying transition separated by about 1.5 eV from a weaker higher state. Furthermore, despite the polyenelike structure of the two molecules, the correlation effect due to single and double configuration interaction is found to bring about a comparable lowering of the energy levels of the ground and the first excited state. In other words, there is no ''overcorrelation'' of the ground state, in sharp contrast to SDCI polyene calculations. It is understood that, in polyenes, while single and double excitation configurations provide an adequate account of correlation for the ground state they do not provide a sufficiently complete description of electron correlation in the one-photon excited states. Higher multiple excitation configurations are needed in order to achieve a

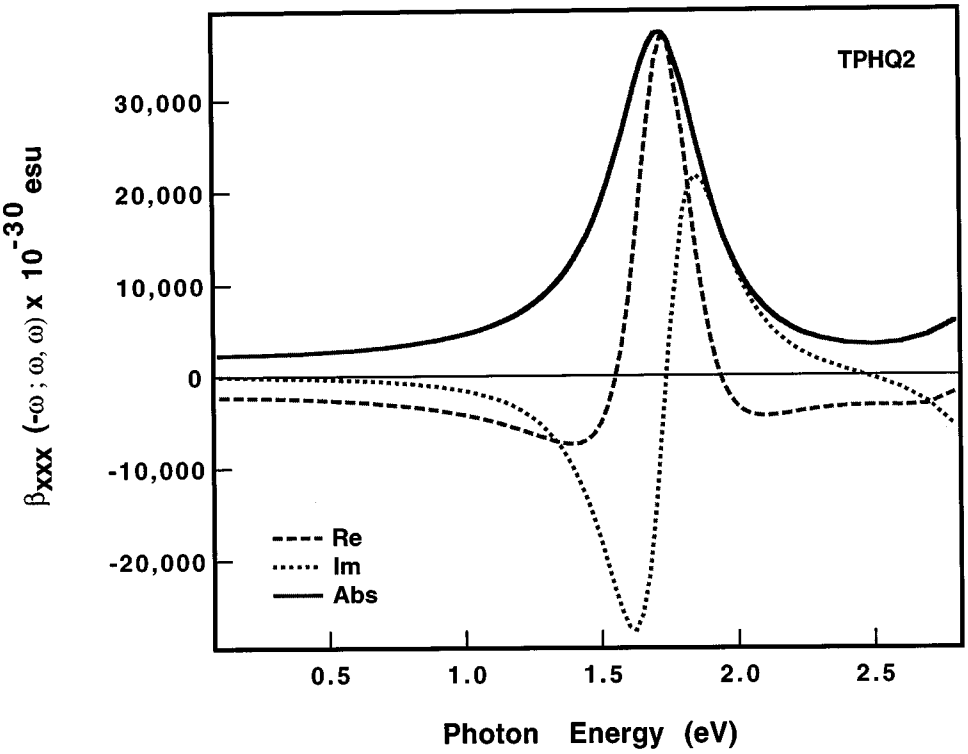

FIG. 7. Calculated SDCI dispersion curves of $\beta_{xxx}(-\omega;0,\omega)$ for TPHQ2: real part (dashed); imaginary part (dotted); $|\beta_{xxx}|$ (solid).

comparably accurate description of the one-photon excited states. A configuration interaction limited to single and double excitation configurations would, therefore, produce a relatively larger lowering of the ground-state energy level compared to that observed for the one-photon excited states. The present calculations suggest, therefore, that SDCI calculations are equally adequate for both the ground and the one-photon excited states of dipolar-quinoid molecules.

Second-order nonlinear susceptibilities have also been calculated for DCNQI and TPHQ2. The calculations for DCNQI are found to be in excellent agreement with dc field-induced second-harmonic-generation dispersion measurements of DCNQI in solution and in Langmuir-Blodgett films. The analysis of the intermediate calculated terms shows that while there are several significant contributing states, the magnitude and sign of the observed second-order nonlinearity is due mainly to the properties of the first excited state; the magnitude of β being mainly due to its low transition energy and relatively large transition moment while the microscopic origin of the negative sign of β lies in the negative sign of its $\Delta\mu$. The calculations for the hypothetical highly conjugated extended quinoid structure TPHQ2 predicts that this molecule will exhibit a negative second-order susceptibility more than an order of magnitude larger in magnitude than that observed in DCNQI. The analysis of the intermediate terms shows that, compared to DCNQI, the first excited state plays a much more dominant role in the contributing virtual-excitation processes due to its lower transition energy, larger transition moment, and larger $\Delta\mu$. The origin of the negative sign of β can be attributed solely to the negative sign of $\Delta\mu$ of the first excited state, as was the case for DCNQI.

ACKNOWLEDGMENTS

This research was generously supported by the U.S. Air Force Office of Scientific Research and the Advanced Projects Research Agency (Grant No. F49620-85-C-0105) and the Pittsburgh Supercomputing Center.

*Present address: Solid State Chemistry Laboratory, Department of Polymer Chemistry, National Institute of Materials and Chemical Research, 1-1 Higashi, Tsukuba, Ibaraki 305, Japan.

[1] S. J. Lalama and A. F. Garito, Phys. Rev. A **20**, 1179 (1979).
[2] J. R. Heflin, K. Y. Wong, O. Zamani-Khamiri, and A. F. Garito, Phys. Rev. B **38**, 1573 (1988).
[3] S. Ramasesha and Z. G. Soos, Chem. Phys. Lett. **153**, 171 (1988).
[4] R. F. Shi, M. H. Wu, S. Yamada, Y. M. Cai, and A. F. Garito, Appl. Phys. Lett. **63**, 1173 (1993).
[5] A. F. Garito, R. F. Shi, and M. H. Wu, Phys. Today **47** (5), 51 (1994).
[6] E. Hendrickx, K. Clays, A. Persoons, C. Dehu, and J. L. Brédas, J. Am. Chem. Soc. **117**, 3547 (1995).
[7] A. F. Garito, K. Y. Wong, and O. Zamani-Khamiri, in *Nonlinear Optical and Electroactive Polymers*, edited by D. Ulrich and P. Prasad (Plenum, New York, 1987).
[8] K. Takahashi, A. Gunji, and K. Akiyama, Chem. Lett. **5**, 863 (1994).
[9] B. J. Orr and J. F. Ward, Mol. Phys. **20**, 513 (1971).
[10] K. Schulten, I. Ohmine, and M. Karplus, J. Chem. Phys. **64**, 4422 (1976).
[11] P. Tavan and K. Schulten, Chem. Phys. Lett. **56**, 200 (1978).
[12] V. Skita, M. Filipkowski, A. F. Garito, and J. K. Blasie, Phys. Rev. B **34**, 5826 (1986).
[13] K. Y. Wong, Ph.D. thesis, University of Pennsylvania, 1986.
[14] P. Boldt, D. Bruhnke, F. Gersen, M. Scholz, P. Jones, and F. Bär, Helv. Chim. Acta **76**, 1739 (1993).
[15] C. C. Teng and A. F. Garito, Phys. Rev. B **28**, 6766 (1983).